THE DYNAMICS OF LIQUEFIED SEDIMENT FLOW UNDERGOING PROGRESSIVE SOLIDIFICATION

S. SASSA
Disaster Prevention Research Institute, Kyoto University, Kyoto 611-0011, Japan

J. MIYAMOTO
Graduate School of Civil Engineering, Kyoto University, Kyoto 611-0011, Japan

H. SEKIGUCHI
Disaster Prevention Research Institute, Kyoto University, Kyoto 611-0011, Japan

Abstract

The propagation of solidified zones in the course of subaqueous liquefied sediment flow is theoretically discussed. The coupled systems of Navier-Stokes equations and consolidation equation are numerically solved under moving boundary conditions, with consideration of the concurrent evolutions of the flow surface as well as of the internally formed interface between the fluid and solidified zones. The analyses for collapse of a body of liquefied soil into ambient fluid under gravity show that the liquefied sediment flow manifests itself as a decelerating gravity flow due to the dynamic interaction between the flowing liquefied soil and the progressively solidified zones in the sediment.

Keywords: dynamics, gravity flow, liquefaction, numerical modelling and analysis, solidification

1 Introduction

Sediment gravity flows have received increasing attention due to the richness in the physics involved and environmental consequences. (Hampton et al.,1996; Simpson, 1997). The importance of pore water pressure in debris flows was pointed out by Iverson (1997). We consider that the changes in pore water pressure may exert significant effects on the process of subaqueous liquefied sediment flow. However, current flow models are mostly depth-averaged ones and cannot describe fully the process of pore fluid migration that should occur in the flowing sediments. The purpose of this study was to propose a numerical model for predicting the flow dynamics of liquefied granular soil in coastal oceans. Specifically, it presents a workable analysis procedure that can describe the mobility and internal flow structure of the liquefied soil with consideration of solidification. The emphasis of the discussion will be placed on giving insights into how a solidified zone develops in the flow process and interacts with the flowing fluid soil.

The organization of this paper is as follows. A theoretical model for the analysis of subaqueous liquefied sediment flow undergoing solidification will first be presented, based on integrated fluid-dynamics and soil-mechanics approaches. This will be followed by a description of the numerical solution procedure adopted. The performance of the proposed theoretical model will then be examined against a classical gravity flow problem. The predicted characteristics of the gravity flow of liquefied sediments will be discussed in detail.

2 Theory for Subaqueous Liquefied Sediment flow with Solidification

2.1 PROBLEM DEFINITION

Consider a body of granular soil in coastal oceans that has just undergone liquefaction under the action of earthquake shaking or wave loading.   The liquefied sediment with a mass density ρ_2 will start collapsing into the ambient fluid with a mass density ρ_1 under gravity. The depth of the ambient fluid (water) is assumed here to be constant in the course of flow. A snapshot of the flowing entire system under consideration is schematically shown in Fig.1. In the course of the liquefied sediment flow, the solidification should occur from the bottom of the liquefied soil layer and develop such that the solidification front, *Zs*, will progress upwards.

Before going into the formulation of the flow and solidification processes, let us note that the pore pressure *p* at a generic point in the sediment may be divided into two components. That is to say,

$$p = p_s + p_e \tag{1}$$

where p_s is the hydrostatic pressure which is expressed as $p_s = \rho_1 g(h\text{-}z)$, and p_e represents the excess pore pressure due to contractancy (i.e., tendency for volume reduction under shearing) of the sediment.
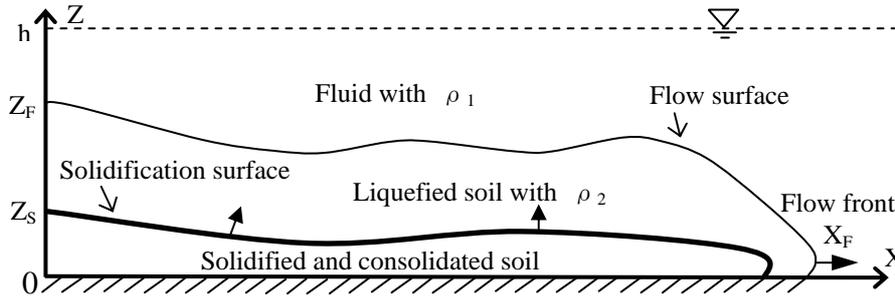
Figure 1.   Problem definition for subaqueous liquefied flow

2.2 FORMULATION FOR THE DOMAIN OF LIQUEFIED FLOW

The liquefied soil is idealized as being a heavy viscous fluid with a mass density $\rho_2 >$ ρ_1 (Fig.1).   For the purpose of non-dimensional formulation, let us denote a reference length as *H* and a reference velocity as $U_r = \sqrt{gH}$. The non-dimensional time *T* may then be expressed as $U_r t/H$ and the non-dimensional excess pore pressure P_e may be expressed as $p_e/(\rho_2 - \rho_1)U_r^2$. It is important here to note that the boundary conditions on the flow surface can be described by $P_e = 0$, with reference to equation (1). The two-dimensional system of Navier-Stokes equations, considering the effect of the excess pore pressure P_e , for describing the dynamics of the subaqueous liquefied flow may then be expressed as:

$$\frac{\partial U}{\partial X} + \frac{\partial V}{\partial Z} = 0 \tag{2}$$

$$\frac{\partial U}{\partial T} + U \frac{\partial U}{\partial X} + V \frac{\partial U}{\partial Z} = -\frac{\rho_2 - \rho_1}{\rho_2} \frac{\partial P_e}{\partial X} + \frac{1}{R_e}\left(\frac{\partial^2 U}{\partial X^2} + \frac{\partial^2 U}{\partial Z^2} \right) \tag{3}$$

$$\frac{\partial V}{\partial T} + U \frac{\partial V}{\partial X} + V \frac{\partial V}{\partial Z} = -\frac{\rho_2 - \rho_1}{\rho_2} \frac{\partial P_e}{\partial Z} + \frac{1}{R_e}\left(\frac{\partial^2 V}{\partial X^2} + \frac{\partial^2 V}{\partial Z^2} \right) - \frac{\rho_2 - \rho_1}{\rho_2} \tag{4}$$

Here $U = u/U_r$ is the non-dimensional velocity in the X-direction, $V = v/U_r$ is the non-dimensional velocity in the Z-direction and R_e is the Reynolds number as expressed by HU_r/ν where ν is the kinematic viscosity of the flowing liquefied soil.

2.3 FORMULATION FOR THE DOMAIN UNDERGOING SOLIDIFICATION

The process of solidification in the course of the liquefied flow may be described by the two-dimensional equation of consolidation. Let K_x and K_z be the Darcy permeability coefficients in the X and Z-directions. They are non-dimensionalized by dividing by U_r. Let M be the constrained modulus of the soil skeleton, which is non-dimensionalized by dividing by $(\rho_2 - \rho_1)U_r^2$. Then the storage equation reads

$$\frac{\partial(\sigma_m - P_e)}{\partial T} = -\frac{\rho_2 - \rho_1}{\rho_1} M \cdot \left(K_x \frac{\partial^2 P_e}{\partial X^2} + K_z \frac{\partial^2 P_e}{\partial Z^2} \right) \tag{5}$$

where σ_m is the non-dimensional mean total stress of the solidifying sediment. Note here that the value of the constrained modulus M should increase with increasing effective confining pressure. With reference to Sassa et al.(2001), we adopt the following simple relationship :

$$M = (Z_s - Z) \cdot M_r \quad \text{for} \quad 0 \le Z \le Z_s \tag{6}$$

where M_r is the reference value of M for the sediment having a non-dimensional thickness of unity.

3 Numerical Solution Procedure Considering Two Moving Boundaries

We will subsequently describe the numerical solution procedure pertaining to the entire system under consideration. Note that the locations of the flow surface as well as the solidification surface are unknowns that should be worked out in the solution procedure for the process of flowage (Fig.1).

The Navier-Stokes equations (3) and (4) together with the equation of continuity (2) may be solved using a finite-difference method. Specifically, a simplified MAC method (Amsden and Harlow,1970) in terms of a staggered rectilinear grid is applied, and the Poisson equations regarding the excess pore pressures P_e are solved using the Gauss-Jordan method. For the purpose of identifying the moving interface between the ambient fluid (water) and the liquefied soil, we adopted the volume-of-fluid (VOF) technique (Hirt and Nichols, 1981). It should also be noted that an efficient volume-advection scheme (Hamzah, 2001) is used in the present study to ensure the conservation of mass in the course of the liquefied flow.

The development of the moving interface between the liquefied soil and the internally

formed zone of solidified soil can be predicted, based on equation (5), by making use of the VOF technique. Namely, the solidification part is treated here as an obstacle to the flowing liquefied soil, such that the velocity in the solidified sediment becomes equal to zero. This assumption may be justifiable, since the solidified zone should have a much higher stiffness and frictional resistance compared with the liquefied soil.

The analysis procedure developed in this study may be summarized as follows:
(A) Assume a thin transition layer, which has zero effective stress but has a marginally discernable stiffness, at the bottom of the liquefied soil.
(B) Solve equations (2)-(4) in the liquefied region above the transition layer.
(C) Solve equation (5), by using the implicit finite-difference method, in the transition layer under the predicted liquefied flow.
(D) If the effective stress increment in the transition layer becomes positive, then identify it to be a consolidated layer and shift a transition layer to the level immediately above the consolidated layer.
(E) Correct the slope of the solidification surface if necessary, so as not to exceed the critical friction angle adopted.
(F) Continue the steps (B)-(E) until the targeted time. Note that the transition layer in (C) represents now the transition layer as well as the consolidated layer developed.

The numerical solution procedure described above makes it possible to predict how the liquefied flow develops along with the solidification and consolidation processes, and how the complex flow structure ensues.

4 Calibration of the Proposed Numerical Analysis Procedure against a Dam-break problem

We will subsequently check the validity of the proposed numerical analysis procedure against a dam-break problem in which a column of water in air collapses under its own weight. The problem definition may be described as follows: a) A single-phase material is used with the mass density ρ_2 equal to unity. b) No solidification is introduced. c) No ambient fluid is present such that $\rho_1 = 0$. The initial height to length ratio of the column as denoted by Z_{F0}/X_{F0} is equal to 2.0. The Reynolds number R_e is assumed to be 10^5. The predicted time history of the head of the gravity flow, X_F, is shown in Fig. 2. The experimental results of Martin and Moyce (1952) are also plotted in this figure. It is seen that the predicted performance compares favourably with the observed flow behaviour, validating the proposed analysis procedure.
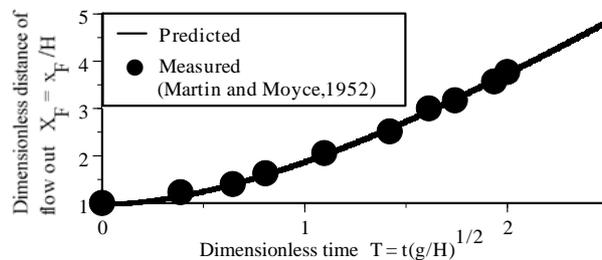
Figure 2. Predicted and measured time histories of the location of the head of gravity flow over a horizontal plane

5 Predicted Features of the Gravity Flow of Liquefied Sediments

This section will discuss the dynamics of gravity flow of liquefied sediments as predicted from the proposed theoretical model. The material parameters used in the analysis are summarized in Table 1. Note that the parameter ϕ represents a critical friction angle adopted for a solidified soil.

Table 1. Material parameters used in the proposed theoretical model

R_e	K_x	K_z	M	ϕ	ρ_1	ρ_2
100000	0.0001	0.0001	400.0	40.0	1.0	2.0

5.1 STARTING CONDITIONS

Consider the situation where a rectangular body of liquefied soil is supported by a pair of smooth vertical wall in water. With one side of the walls being instantly removed, the liquefied sediment starts flowing into the ambient water under gravity. Note here that the solidification is not introduced at the other end of the wall.

5.2 PROGRESSIVE NATURE OF SOLIDIFICATION

The predicted changes in the configuration of the liquefied sediment are illustrated in Fig. 3 for four different dimensionless times. At T = 0, the solidification surface coincides with the bottom of the liquefied sediment. It is seen that at T= 0.75 the liquefied sediment has been collapsing and the solidification front has progressed upwards to a maximum dimensionless height of 0.3. The liquefied sediment then undergoes a significant flow deformation, resulting in a flow-out distance X_F equal to 3.3 at T= 3.0. The solidified zone has developed further upwards and laterally. It is interesting to note that the front of the solidification surface has reached the flow surface front at T=3.0, making the flowage velocity slow down.   The liquefied flow becomes markedly elongated at T = 7.5. It is also interesting to observe that at T=7.5, the solidified region has developed in a wavy fashion.
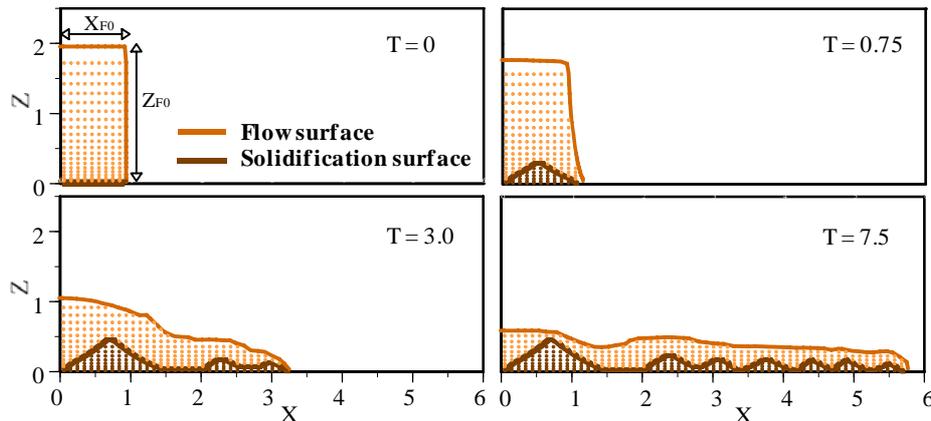
Figure 3. Predicted temporal changes of flow and solidification surfaces

The predicted time history of the ratio of the solidified volume V_{SC} to the total volume of the sediment V is plotted in Fig. 4(a). It is evident that the V_{SC}/V-ratio increases with time, giving rise to the V_{SC}/V-value as high as 0.5 at T = 8. The consequence of the progressive solidification on the flow process can be clearly seen in Fig. 4(b) where the predicted time history of the head of the gravity flow X_F is plotted. For the purpose of comparison, the predicted performance for the fluid gravity flow without solidification is also shown in Fig. 4(b). It is seen that in the case of the fluid gravity flow without solidification, a simple form of accelerating flow takes place. By contrast, in the liquefied sediment flow with solidification, the accelerating flow occurs only at the initial stage of the flow, and deceleration becomes noticeable at and after T = 2.8. In fact, the subsequent flow process is characterized by the repeated stages of flow and intermittent standstill, resulting in the eventual stoppage of the flow at T = 8 or thereabouts.   It is important to remark that the flow undergoes a freezing process when a part of the internally developed solidified zone has extended to the head of the flowage, as shown in Fig. 3(c). This behaviour emphasizes that the freezing of the flow can occur not by the rheological properties of a single-phase fluid soil, but by the salient physics of the two-phase material. This statement will be reinforced subsequently.
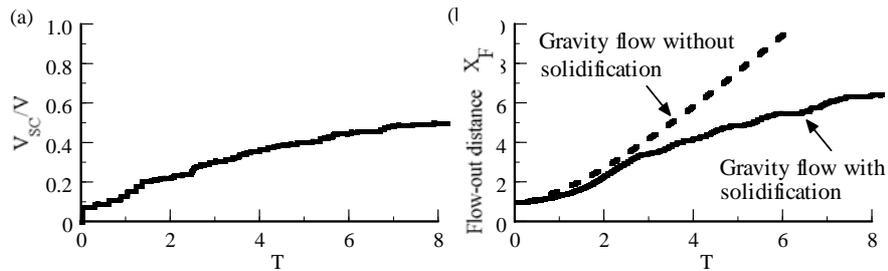
Figure 4. Predicted time histories of (a) the solidified volume ratio and (b) the location of the flow surface front

5.3 INTERNAL FLOW STRUCTURES

5.3.1 *Excess Pore Pressure Distributions*
The predicted excess pore pressure distributions at T=7.5 are shown in Fig. 5(a). Note in this figure that the scale in the vertical direction Z is elongated for illustrative purposes. It is seen that the excess pore pressure takes the highest value of 0.9 at the point X=0.5,Z=0 which corresponds to the center of the base of the initial configuration of the liquefied sediment. The pressure gradients in the Z-direction are negative in most areas, indicating the occurrence of the upward seepage flow in the solidifying sediment.
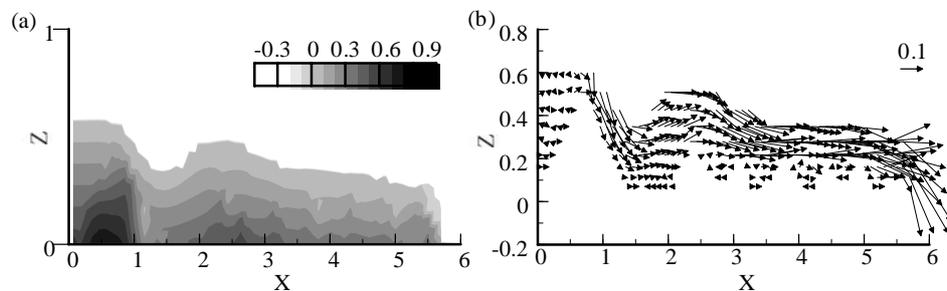
Figure 5. Predicted distributions of (a) excess pore pressures and (b) velocity vectors

5.3.2 *Velocity Vector Field*

The predicted velocity vector field at T= 7.5 is plotted in Fig. 5(b). Note that the solidified regions have zero velocity. A close examination of the velocity vector field shows the importance of the strong interaction between the flowing liquefied soil and the solidified sediment. In fact, clock-wise fluid motions take place in the depressions of the solidified sediment. This behaviour is compatible with the decelerating flow pattern that is effected (cf. Fig. 4(b)).

5.3.3 *Effective Stress Profile*

The predicted profile of the mean total stress σ_m subtracting the hydrostatic pressure P_s is shown in Fig. 6 together with the excess pore pressure P_e against Z profile. The vertical profile at a station X = 2.4 for T = 7.5 is taken up here. Note that the hatched area in Fig. 6 represents the mean effective stress developed, as defined by σ_m-P_e. The predicted performance tells us that while the region between the flow and solidification surfaces maintains a liquefied state such that $\sigma_m = P_e$, there are significant developments of the effective stress in the region that has been solidified in the course of flowage.
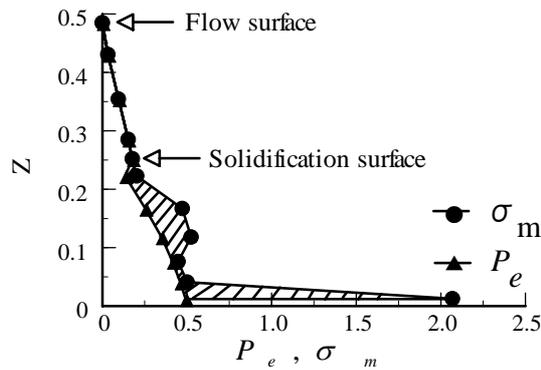
Figure 6.   Predicted vertical profiles of excess pore pressure P_e and mean total stress σ_m with depth Z

6 Discussion

For practical implications, the predicted relationships between the flow-out distance and the volume of liquefied sediment are shown in Fig. 7 in terms of physical dimensions.
This figure was constructed as follows. The dimensionless distance of flow-out of the liquefied sediment with $X_{F0}=1$ and $Z_{F0} = 2.0$ as discussed in Section 5, was equal to $X_F= 6$ (Fig. 4). With this in mind, we dimensionalized the flow-out distance as $x_F = X_F H$ and the volume of liquefied sediment as $V= X_{F0} Z_{F0} H^2$. The reference length H was varied from 1 to 7×10^3m. It is evident that the flow-out distance increases markedly with the volume of the liquefied sediment (gravity flow with solidification). This behaviour may provide a key for better understanding of very large submarine gravity flows as reported in Hampton et al. (1996).

The flow-out distance predicted without solidification is also shown in Fig. 7, as represented by the hatched area above a dotted line. In the case of the gravity flow without solidification, we overpredicts the flow-out distance by three times or even more, because of the absence of physics that is relevant to the two-phase granular material.
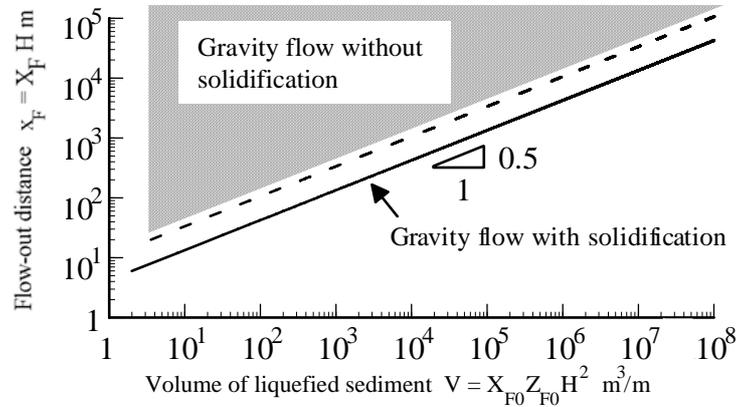
Figure 7. Predicted flow-out distances against the volume of liquefied sediments

7 Conclusions

A workable analysis procedure for describing the dynamics of subaqueous liquefied sediment flow undergoing progressive solidification has been developed, based on the integrated systems of the Navier-Stokes equations for a fully liquefied soil and the equation of consolidation for a solidifying soil.   The characteristics of the liquefied gravity flow as predicted from the proposed theoretical model may be summarized as follows.   (a) In the course of the liquefied flow, a solidified region is formed at the bottom of the liquefied soil and then extends upward and laterally. (b) The progressive nature of the solidification has a profound influence on the process of flowage, giving rise to a decelerating flow regime.   (c) The internal flow structures predicted are worth close examination. Indeed, the predicted significant development of effective stress in the course of the liquefied sediment flow is interesting, calling for careful experimentation regarding flow deceleration.

REFERENCES

Amsden, A.A. and Harlow, F.H., 1970. A simplified MAC technique for incompressible fluid flow calculations. J. Comput.Phys., 6: 322-325.

Hampton, M.A., Lee, H.J. and Locat J. 1996. Submarine landslides. Reviews of Geophysics, 34: 33-60.

Hamzah, M.A., 2001. *Numerical simulations of tsunami pressure acting upon coastal barriers on wet and dry lands*. Dr.Eng. thesis, Kyoto University, 101p.

Hirt, C.W. and Nichols, B.D., 1981. Volume of fluid (VOF) method for the dynamics of free boundaries. J. Comput. Phys., 39: 201-225.

Iverson, R.H., 1997. The physics of debris flows. Reviews of Geophysics, 35: 245-296.

Martin, J.C. and Moyce, W.J., 1952. An experimental study of the collapse of liquid columns on a rigid horizontal plane. Philos.Trans.R.Soc.London Ser.A, 244: 312-324.

Sassa, S., Sekiguchi, H. and Miyamoto, J., 2001. Analysis of progressive liquefaction as a moving boundary problem. Géotechnique, 51: 847-857.

Simpson, J.E., 1997. *Gravity Currents in the Environment and the Laboratory*. Second Edition. Cambridge University Press. 244p.